

# Multinode State Transfer and Nonlocal State Preparation via a Unidirectional Quantum Network

Hao Ai,<sup>1</sup> Ying-Yü Fang<sup>✉,1</sup>, Cheng-Rui Feng<sup>✉,1</sup>, Zhihui Peng,<sup>2</sup> and Ze-Liang Xiang<sup>✉,1,\*</sup>

<sup>1</sup>*School of Physics, Sun Yat-sen University, Guangzhou 510275, China*

<sup>2</sup>*Key Laboratory of Low-Dimensional Quantum Structures and Quantum Control of Ministry of Education, Key Laboratory for Matter Microstructure and Function of Hunan Province, Department of Physics and Synergetic Innovation Center for Quantum Effects and Applications, Hunan Normal University, Changsha 410081, China*

(Received 12 December 2021; revised 3 March 2022; accepted 15 April 2022; published 12 May 2022)

Quantum networks with the ability to coherently transfer quantum states between different nodes open up possibilities for upscaling quantum technologies. In this work, we propose a theoretical protocol to implement the multinode state transfer and nonlocal state preparation in a one-dimensional network consisting of many quantum nodes coupled to a common unidirectional channel. By time-dependently modulating the coupling strength between the nodes and the channel, a quantum state stored in one node can be distributed to the other nodes through the channel, while a series of dark-state conditions ensure a desired final state. This protocol can also be used to prepare nonlocal entanglement states of these nodes, such as the  $W$ -type state. Importantly, it can be realized in various quantum platforms with currently available technologies.

DOI: 10.1103/PhysRevApplied.17.054021

## I. INTRODUCTION

A quantum network can connect spatially discrete quantum devices, such as quantum memories [1–4], routers [5,6], and processors [7] for scalable quantum computation [8], remote operation [9], and secure communication [10]. No matter how complicated a quantum network is, it can be abstracted into a structure of multiple nodes connected with channels. Quantum information is stored and processed in nodes while channels permit the information to coherently transfer between them [11]. The nonlocality gives a quantum network distinct advantages over a classical one [12,13].

In the last decades, many efforts have been devoted to finding a suitable channel to connect spatially discrete nodes and to finally constructing a quantum network [10,14–23]. One promising candidate is the bosonic waveguide, which can link spatially discrete quantum nodes via flying photons [17–20], just like a highway connecting cities. In order to perfectly transfer a quantum state between two quantum nodes in such a system, a time-dependent modulation of the flying photon in both emitting and absorbing processes is necessary [20,24–28]. This modulation can be realized by employing two-level atoms or harmonic oscillators embedded in nodes with tunable couplings. If a so-called dark-state condition [20], which ensures that the photon can be completely absorbed by the

second node without any reflection, is fulfilled in the whole process, perfect quantum transmission can occur. Specifically, this system can be immune to thermal noise when harmonic oscillators are employed as the nodes [24]. Such state-transfer protocols usually require the channel to be unidirectional, which is achievable through chiral interactions [29,30], topological edge states [31–33], or quantum isolators [34]; however, a bidirectional channel can also work well when a more complicated condition is satisfied [25]. Importantly, one can carry out these protocols in existing experimental platforms, such as superconducting circuits [35–41], optomechanical systems [28,42–45], spin vacancies [46–52], quantum dots [53–55], and trapped ions [56]. Recently, several important experiments concerning quantum state transfer have also been realized [35,57].

There have been some preliminary discussions about the multinode quantum network in previous works [28,45]; however, most of these discussions only focused on the state transfer between two nodes in the network. In this work, we propose a protocol to implement the multinode state transfer and nonlocal state preparation in a one-dimensional network, which contains a one-node emitter and a multinode receiver linked by a unidirectional channel. This protocol can transfer a quantum state from the emitter to a target receiving node and generate some specific entanglement states in the receiver, like Bell states  $|\Psi^\pm\rangle$  and  $W$ -type states [58]. Furthermore, with the help of projective measurements, it can also be applied to the generation of Bell states  $|\Phi^\pm\rangle$  and

\*xiangzliang@mail.sysu.edu.cn

Greenberger-Horne-Zeilinger (GHZ) states [58–60]. All of these provide possibilities to develop more functional and powerful quantum networks. The key to the protocol is the designed modulation of the coupling between the nodes and the unidirectional channel. The transfer and preparation process is described by quantum Langevin equations and input-output relations, while the pulse shapes of the time-dependent coupling are obtained from a series of extended dark-state conditions. Since the protocol is not restricted to any specific quantum systems in our study, it may be realized in various quantum platforms.

The remainder of the article is organized as follows. We firstly describe the simplified model of the quantum network in Sec. II. In Sec. III, we demonstrate how to generate multimode entanglement in the protocol and give two examples: Bell states  $|\Psi^\pm\rangle$  and  $W$ -type states. The method of generating Bell states  $|\Phi^\pm\rangle$  and GHZ states is given in Sec. III C. After that, we analyze imperfections of the protocol in Sec. IV, and discuss the experimental feasibility in Sec. V based on two different quantum systems. Finally, in Sec. VI we present our concluding remarks.

## II. MODEL OF A 1D NETWORK

Here we discuss the one-dimensional (1D) quantum network illustrated in Fig. 1, where the working frequencies of nodes connected to the channel are assumed to be the same. The unidirectional channel is treated as a waveguide with a continuous spectrum. The Hamiltonian of the total system can be written as

$$H_{\text{total}} = H_W + \sum_j H_j + \sum_j H_{I,j}, \quad (1)$$

where  $H_W$  and  $H_j$  denote the Hamiltonians of the waveguide and the  $j$ th node, respectively, and  $H_{I,j}$  describes the interaction between the  $j$ th node and the waveguide. We first ignore the effects of thermal noise and propagation loss in the waveguide, which will be discussed in Sec. IV. For simplicity, each node here is assumed to be a harmonic

oscillator. Note that the following discussion is also valid for the case where nodes are replaced by two-level systems and the whole network involves only a single excitation at any time [61]. Under the rotating-wave approximation,  $H_j$  and  $H_{I,j}$  can be written as

$$\begin{aligned} H_j &= \hbar\omega_0 a_j^\dagger a_j, \\ H_{I,j} &= i\hbar \int_{\omega_0-\Delta\omega}^{\omega_0+\Delta\omega} d\omega g_j(\omega, t)(a_j B_{\omega,j}^\dagger - a_j^\dagger B_{\omega,j}), \end{aligned} \quad (2)$$

where  $a_j^\dagger$  ( $a_j$ ) is the creation (annihilation) operator of the  $j$ th node,  $\omega_0$  is the frequency of these nodes, and  $B_{\omega,j}$  ( $B_{\omega,j}^\dagger$ ) is the annihilation (creation) operator of the waveguide mode nearing node  $j$ . The cavity-waveguide coupling is valid in a small bandwidth around  $\omega_0$ , so the coupling strength  $g_j(\omega, t)$  approximately equals  $g_j(\omega_0, t)$ . Thus, we can rewrite  $g_j(\omega, t)$  as  $g_j(t)$ , which means that the time-dependent coupling strengths are independent of the frequency in this range.

Using the Markov approximation, the evolution of annihilation operators  $a_j$  can be described by a series of quantum Langevin equations (QLEs) [62],

$$\dot{a}_j(t) = -i\omega_0 a_j(t) - \frac{1}{2}g_j^2(t)a_j(t) - g_j(t)f_{\text{in},j}(t), \quad (3)$$

where  $f_{\text{in},j}(t)$  is the incoming field for the  $j$ th node,  $f_{\text{in},j}(t) = \int d\omega \exp(-i\omega t)B_{\omega,j}$ . The input-output relations of the nodes are [63]

$$f_{\text{out},j}(t) = f_{\text{in},j}(t) + g_j(t)a_j(t). \quad (4)$$

Detailed derivations of Eqs. (3) and (4) are given in Appendix A. In this one-dimensional network, the incoming field of a node just equals the outgoing field of the node ahead of it with a time delay  $\tau$ , i.e.,  $f_{\text{in},j}(t) = f_{\text{out},j-1}(t - \tau)$ , where  $\tau = L/v_g$  with  $L$  the distance between two nearby nodes and  $v_g$  the group velocity in the waveguide. By

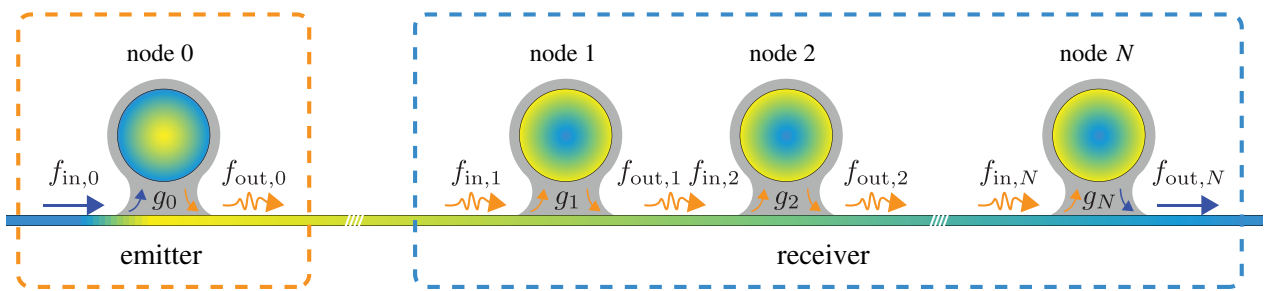


FIG. 1. Schematic of a one-dimensional quantum network, where  $N + 1$  nodes are coupled to a unidirectional waveguide. The first node is the emitter and the other nodes constitute the receiver. The coupling strength  $g_j(t)$  between the  $j$ th node and the waveguide is time dependent. The incoming and outgoing fields of the  $j$ th node are described with  $f_{\text{in},j}$  and  $f_{\text{out},j}$ .

redefining  $f_{\text{out},j}$  and  $a_j$ , this delay  $\tau$  can be eliminated:

$$f_{\text{in},j}(t) = f_{\text{out},j-1}(t). \quad (5)$$

Finally, in a frame rotating with  $\omega_0$ , the dynamics of the entire network can be well described by simplified input-output relations and QLEs at zero temperature (details in Appendix A),

$$f_{\text{out},j}(t) = \sum_{k \leq j} g_k(t) a_k(t), \quad (6)$$

$$\dot{a}_j(t) = - \sum_k \Theta(j-k) g_j(t) g_k(t) a_k(t), \quad (7)$$

where  $\Theta(x)$  is the Heaviside step function with  $\Theta(0) = 1/2$ , and the input noise is ignored for simplicity.

### III. PROTOCOL OF STATE TRANSFER AND PREPARATION

#### A. Two-node state transfer

Our protocol focuses on transferring and distributing quantum information stored in the emitter to implement the state transfer and preparation process on a multimode receiver. The simplest case of quantum state transfer is the two-node one, i.e., a cut-and-paste process from the emitting node to any desired receiving node  $j$ ,

$$(c_1|1\rangle_0 + c_0|0\rangle_0)|0\rangle_j \rightarrow |0\rangle_0(c_1|1\rangle_j + c_0|0\rangle_j). \quad (8)$$

In order to realize such a two-node transfer, some feasible approaches have been studied [20,24,25,28]. In a multinode network, these protocols are also valid; we only need to switch off the coupling between remaining nodes and the channel and then design the modulation of couplings between the concerned nodes and the channel for shaping the flying photon. For example, choosing time-symmetric pulses of coupling strengths  $\{g_0(t), g_j(t)\}$  following  $g_j^2(t_f - t) = g_0^2(t)$ , the whole process can be time symmetric [24,25]. A plot of the time-symmetric process of the state transfer is shown in Fig. 2 with

$$g_j^2(t) = \begin{cases} \frac{g_M^2 \exp[g_M^2(t - t_f/2)]}{2 - \exp[g_M^2(t - t_f/2)]}, & t < t_f/2, \\ g_M^2, & t \geq t_f/2, \end{cases} \quad (9)$$

where  $g_M$  is the maximal coupling strength and  $t_f$  is the time span of this process [28]. Note that a  $\pi$  phase of the receiver will be generated after the process of the state transfer and also state preparation in the following subsections; however, it can be eliminated by applying a phase shift gate.

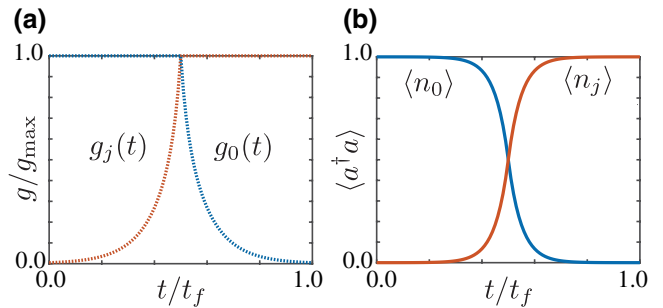


FIG. 2. (a) The pulse shapes of time-symmetric couplings in a quantum state-transfer process between two nodes. (b) The occupation numbers of the emitting node and receiving node during the process. Note that they are time symmetric as well.

#### B. Multinode state preparation

For a receiver containing multiple nodes, the two-node state-transfer protocol can be extended to a multinode information-distribution and state-preparation protocol, which can be used to generate entanglement states, such as Bell states  $|\Psi^\pm\rangle$  and  $W$ -type states. It can also be used to generate Bell states  $|\Phi^\pm\rangle$  and GHZ states after some projective measurements discussed in Sec. III C. In this section, we discuss the generation of Bell states  $|\Psi^\pm\rangle$  and  $W$ -type entanglement states first.

At the beginning, the emitting node is excited to  $|1\rangle$ , and every receiving node is in its ground state  $|0\rangle$ . The aim of this protocol is to then generate an entanglement state of multiple nodes,

$$|1\rangle_0|00\dots\rangle \rightarrow |0\rangle_0 \sum_{j \geq 1} c_j |\dots 1_j \dots\rangle, \quad (10)$$

where  $|\dots 1_j \dots\rangle$  means that only the  $j$ th node is excited while the others are still in the ground state. The amplitudes  $c_j$  are complex and satisfy the normalization relation  $\sum_{j \geq 1} |c_j|^2 = 1$ . In the Heisenberg picture, Eq. (10) is equivalent to  $a_j(t_f) = c_j a_j(0)$ . For example, if the amplitudes  $c_j$  are set equal, i.e.,  $c_1 = c_2 = \dots = c_N = 1/\sqrt{N}$ , the final state of the receiver would become a  $W$ -type state [for a two-node receiver, the  $W$ -type state is just the Bell state  $|\Psi^\pm\rangle = (|01\rangle + |10\rangle)/\sqrt{2}$ ].

To derive the pulse shapes of couplings, we should first obtained the pulse shape of  $g_N(t)$  according to the dark-state condition of the whole system,

$$f_{\text{out},N} = \sum_j g_j(t) a_j(t) \equiv 0, \quad (11)$$

which implies that no photon or information is released at the output side of the channel. Besides dark-state condition (11), we need to introduce the extended dark-state conditions, under which outgoing fields of the  $(j-1)$ th node

are proportional to those of the  $j$  th node,

$$f_{\text{out},j-1}(t) = D_{j-1,j} f_{\text{out},j}(t), \quad (12)$$

where  $D_{j-1,j}$  is a complex function of  $[g_{j+1}(t)/g_j(t)]$ :

$$D_{j-1,j} = \frac{g_{j+1}(t)}{g_j(t)} \frac{c_j}{c_{j+1}} \left( 1 + \frac{1}{D_{j,j+1}} \right) - 1. \quad (13)$$

By defining  $1/D_{N-1,N} = 0$ , which is equivalent to  $f_{\text{out},N} = 0$ , we can calculate other coefficients  $D_{j-1,j}$  through iteration. For simplicity, we can set  $\dot{a}_j(t)/\dot{a}_{j+1}(t) \equiv c_j/c_{j+1}$  to obtain iterative Eq. (13) when we take into account the boundary conditions (see Appendix B)

$$a_j(0)/a_{j+1}(0) = a_j(t_f)/a_{j+1}(t_f) = c_j/c_{j+1}. \quad (14)$$

### 1. Symmetrical pulses

Based on the previous time-symmetrical pulse shape, we can generalize the state-transfer protocol of two nodes to the multinode case. Inspired by the time-symmetrical boundary conditions, we set the pulses  $g_0(t)$  and  $g_N(t)$  to satisfy the relation  $g_0^2(t) = g_N^2(t_f - t)$ . Together with the extended dark-state conditions (12), and the simplified QLEs (7), the following equations of  $g_j(t)$  can be obtained:

$$\left( \frac{D_{j-1,j}}{D_{j-1,j} - 1} - \frac{1}{2} \right) g_j^2(t) = \left( \frac{D_{j,j+1}}{D_{j,j+1} - 1} - \frac{1}{2} \right) g_{j+1}^2(t). \quad (15)$$

Here  $D_{j-1,j}$  is a function of  $(g_{j+1}/g_j)$  shown in Eq. (13), so that all the pulses  $g_j(t)$  for  $j \geq 1$  can be solved by an iterative method. (See Appendix B.)

Let us take the process  $|1\rangle|00\rangle \rightarrow |0\rangle(|10\rangle + |10\rangle)/\sqrt{2}$  for example. The corresponding pulse shapes are depicted in Fig. 3(a), where  $g_2(t)/g_1(t) = 1 + \sqrt{2}$ . The corresponding evolution of the system is shown in Fig. 3(b), where  $c_1$  and  $c_2$  remain equal due to the extended dark-state conditions (12). Another example is the generation of another Bell state  $|\Psi^-\rangle = (|01\rangle - |10\rangle)/\sqrt{2}$ , which is in fact a discussion of the phase property. The pulse shapes are shown in Fig. 3(c) with  $g_2(t)/g_1(t) = \sqrt{2} - 1$  in this case, while the corresponding evolution is shown in Fig. 3(d). (See Appendix B.)

### 2. Numerical asymmetrical pulses

The dark-state condition actually plays the most crucial role in this protocol, rather than the time symmetry of coupling pulses. When the dark-state conditions (12) are satisfied, any shaped flying photon released from the emitter would be distributed as we desire. Hence, a more general way of generating Bell states  $|\Psi^\pm\rangle$  and  $W$ -type states is to initialize the emitting node to  $|1\rangle$ , then produce a pulse of  $g_0(t)$  that can release a flying photon to

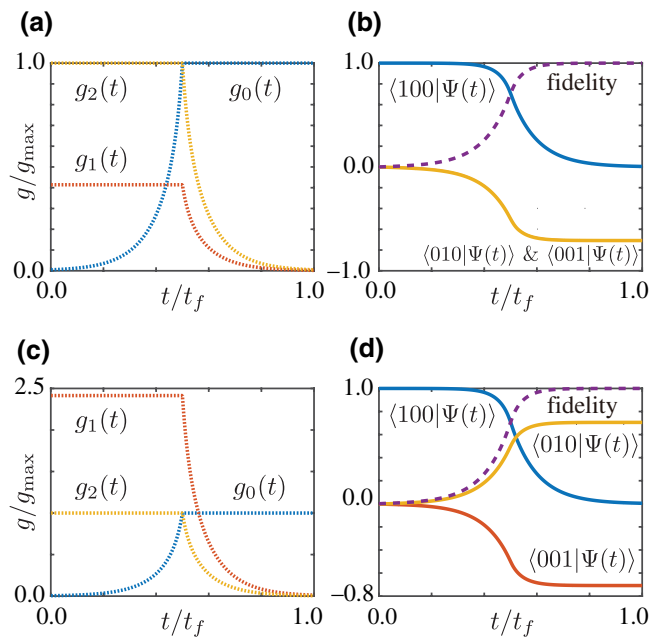


FIG. 3. Symmetrical pulse shapes for preparing two Bell states  $|\Psi^\pm\rangle$ , and the corresponding evolution of the whole network. Panel (a) shows the time dependence of couplings for the generation of Bell state  $|\Psi^+\rangle = (|01\rangle + |10\rangle)/\sqrt{2}$  and (c) shows the time dependence for the generation of  $|\Psi^-\rangle = (|01\rangle - |10\rangle)/\sqrt{2}$ . In both (a) and (c), the pulse shapes of the first node  $g_0(t)$  and the last one  $g_2(t)$  are symmetric with respect to  $t = t_f/2$ , and  $g_1(t)$  is proportional to  $g_2(t)$ . The simulation results of the evolution in two different processes are shown in (b) and (d), respectively, where curves of the fidelity and the projection to the initial state  $\langle 100|\Psi(t)\rangle$  are also symmetric about  $t = t_f/2$ .

the channel with the expected shape, and finally apply a series of pulses  $g_j(t)$ , which can be calculated numerically, to receive the desired state.

Since the state is ideally initialized to  $|100\dots\rangle$ , QLEs and output fields can be written as

$$\dot{A}_j(t) = \sum_k g_k(t) g_j(t) A_k(t) \Theta(j - k), \quad (16)$$

$$F_{\text{out},j}(t) = \sum_{k \leq j} g_k(t) A_k(t), \quad (17)$$

where  $A_j(t)$  is the amplitude of base  $|\dots 1_j \dots\rangle$ , satisfying  $A_j(t_f) = c_j$ . Then the dark-state conditions (12) become

$$F_{\text{out},j-1}(t) = D_{j-1,j} F_{\text{out},j}(t). \quad (18)$$

Note that  $D_{j-1,j}$  is a function of  $\{g_{k+1}(t)/g_k(t) \mid k = 1, \dots, N-1\}$  given by iterative Eq. (13). So Eq. (18) implies the relation between  $\{A_j(t) \mid j = 0, \dots, N\}$  and  $\{g_{k+1}(t)/g_k(t) \mid k = 1, \dots, N-1\}$ . At a certain time  $t$  with a given  $g_0(t)$ , we can obtain  $\{g_j(t) \mid j = 1, \dots, N\}$  as a function of the amplitudes  $\{A_k(t) \mid k = 0, \dots, N\}$  by solving Eq. (18) numerically. Substituting them into Eq. (16),

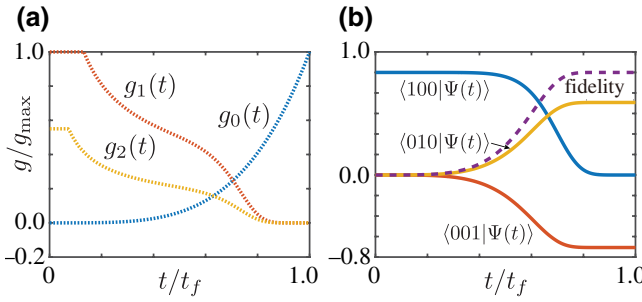


FIG. 4. Asymmetrical pulses obtained by numerical simulation for preparation of state  $|\Psi^-\rangle$  and the corresponding evolution of the network. (a) The artificially regulated coupling strengths  $g_j(t)$ . (b) Evolution of the network demonstrated through time curves of the fidelity and the projections to different states.

we obtain a series of ordinary differential equations concerning  $\{A_k(t) \mid k = 0, \dots, N\}$ . Then we solve them and get the values of  $A_j(t)$  and  $g_j(t)$  for any  $j$  and  $t$ . Considering the feasibility, we set  $g_j(s) (j \geq 1, s \approx 0)$  to be constants, which have no impact on the evolution, because the amplitudes of states except the initial state are particularly small in the beginning. An example of generating  $|\Psi^-\rangle = (|01\rangle - |10\rangle)/\sqrt{2}$  is shown in Fig. 4.

### C. The generation of GHZ entanglement

Besides Bell states  $|\Psi^\pm\rangle = (|01\rangle \pm |10\rangle)/\sqrt{2}$  and  $W$ -type states, if the nodes are harmonic oscillators, this protocol may also be used to generate Bell states  $|\Phi^\pm\rangle = (|11\rangle \pm |00\rangle)/\sqrt{2}$  or GHZ-type states with the help of projective measurements.

In order to illustrate the idea clearly, we first consider a toy model, which consists of three oscillators arranged in a line. In this model, the adjacent oscillators are coupled with an identical coupling strength  $g$ . The interaction Hamiltonian can be written as

$$H_{\text{int}} = g(a_1^\dagger a_2 + a_1 a_2^\dagger) + g(a_2^\dagger a_3 + a_2 a_3^\dagger), \quad (19)$$

where  $a_1, a_2, a_3$  are annihilation operators of the oscillators. If the oscillators are initialized to  $|\psi\rangle = |020\rangle$ , i.e., only the second oscillator is emitted by two photons, the state after half-period evolution is

$$|\psi'\rangle = |0\rangle_2 \left( \frac{1}{2} |20\rangle_{13} + \frac{1}{\sqrt{2}} |11\rangle_{13} + \frac{1}{2} |02\rangle_{13} \right), \quad (20)$$

where the subscripts indicate oscillators' serial numbers; see Fig. 5(a). The effect of this process is the same as an optical beam splitter. Two photons leak from oscillator 2 and either of them could go left or right. Thus, the possibility of both photons going left (right) and generating  $|20\rangle_{13}$  ( $|02\rangle_{13}$ ) is  $1/4$ , while the probability of two photons going in different directions and generating  $|11\rangle_{13}$  is  $1/2$ .

In our protocol with a unidirectional channel, a similar but aperiodic process can be implemented by using a series of equally distributing pulses, i.e.,  $|c_1|^2 = |c_2|^2 = \dots |c_N|^2 = 1/N$  in Eq. (10). For a two-node receiver, equally distributing pulses may generate Bell states  $|\Phi^\pm\rangle = (|11\rangle \pm |00\rangle)/\sqrt{2}$  with the help of projective measurements through the following steps. First, the emitter is initialized to  $\sqrt{1/3}|0\rangle \mp \sqrt{2/3}|2\rangle$ , and then the receiver state will be  $|\Phi'\rangle = \sqrt{1/3}|00\rangle \pm \sqrt{1/3}|11\rangle \pm \sqrt{1/6}|20\rangle \pm \sqrt{1/6}|02\rangle$  after the process with equally distributing pulses; see Fig. 5(b). Then  $|\Phi'\rangle$  can be concentrated to Bell state  $|\Phi^\pm\rangle$  with projective measurements [64]. For an  $N$ -node receiver, equally distributing pulses can generate GHZ states by initializing the emitter to  $A_0|0\rangle \mp A_N|N\rangle$ , where  $A_0 = \sqrt{F(N)/2}$  and  $A_N = \sqrt{1 - |A_0|^2}$  with  $F(N)$  the success rate of projective measurements for one process, i.e.,

$$F(N) = \frac{2N!/N^N}{N!/N^N + 1}, \quad (21)$$

which follows from the identical principle because of the indistinguishability of photons. Although the purification process may not succeed once, the generation of GHZ states can be ensured by repeating this process. The average number of repetitions, i.e., the cost of generating such a GHZ state, depends on the receiving-node number, which is depicted in Fig. 5(c).

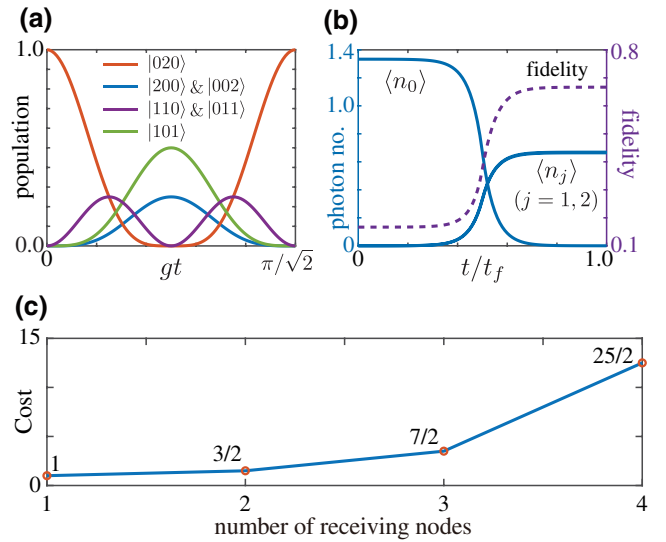


FIG. 5. (a) The evolution of the populations of each oscillator in the toy model, which is initialized to  $|020\rangle$ . (b) Occupation numbers of both receiver nodes and the fidelity when generating a Bell state  $|\Phi^+\rangle = (|00\rangle + |11\rangle)/\sqrt{2}$ . The emitter is initialized to  $\sqrt{1/3}|0\rangle_0 - \sqrt{2/3}|2\rangle_0$  while the fidelity is  $2/3$  after the process. (c) The relation between the generating cost and the number of receiving nodes.

#### IV. IMPERFECTIONS

Considering experimental conditions, we briefly analyze three sources of imperfections (the input thermal noise, the propagation loss, and the loss from the nodes, e.g., spontaneous emission) in this section. The input thermal noise added to the emitter  $f_{\text{in},0}$  ( $\langle f_{\text{in},0}^\dagger f_{\text{in},0} \rangle = N_{\text{th}}$ ) can be expressed with the thermal photon number  $N_{\text{th}} = (e^{\hbar\omega_0/k_B T} - 1)^{-1}$  at temperature  $T$ . Figure 6(a) shows the imperfect generating process of  $(|01\rangle + |10\rangle)/\sqrt{2}$  when  $N_{\text{th}} = 0.1$ . An evident method of suppressing the thermal noise is to keep the system in an effective low-temperature environment, i.e.,  $N_{\text{th}} \rightarrow 0$ . For example, current dilution refrigerators can reach a base temperature of 10 mK, which is equivalent to an occupied thermal photon number  $N_{\text{th}} \approx 1 \times 10^{-2}$  in a superconducting qubit with a typical working frequency  $\omega_0 = 2\pi \times 6$  GHz, and the corresponding fidelity of the above process is nearly 99%. When the temperature is low, one can also reduce the influence of the input noise by using harmonic oscillators as nodes, instead of two-level systems, because linear systems would have better noise immunity compared to nonlinear systems in this protocol [24], as shown in Fig. 6(b).

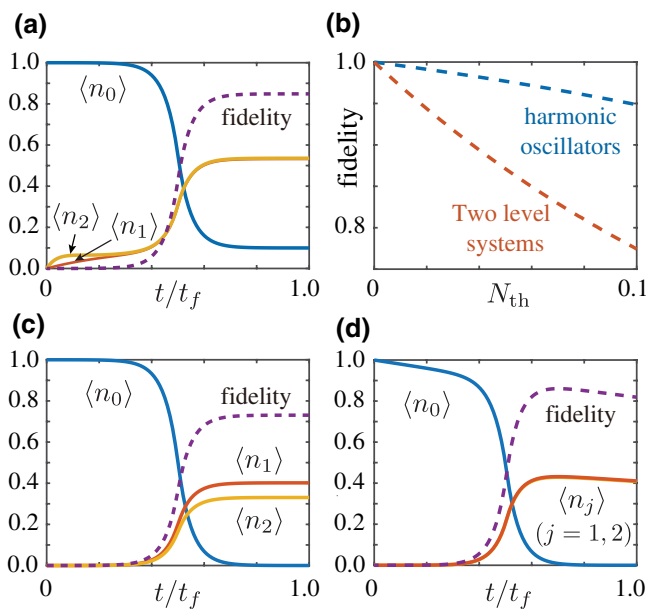


FIG. 6. The effects of thermal noise and propagation loss in this protocol. (a) The evolution of average occupation numbers  $\langle n_j(t) \rangle$  and the fidelity when  $N_{\text{th}} = 0.1$ . (b) Relations between the average fidelity and  $N_{\text{th}}$  for harmonic oscillators and two-level systems. We find that the former ones can have better antinoise performance at lower temperature. Note that the fidelity is the average value of generating states  $|01\rangle, |10\rangle, (|01\rangle \pm |10\rangle)/\sqrt{2}$ . (c) The evolution of average occupation numbers  $\langle n_j(t) \rangle$  and the fidelity with a total loss of the waveguide  $\kappa = 0.9$ . (d) A simulation considering quantum information loss from the nodes when  $g_{\text{env}} = g_{\text{max}}/10$  and  $N_{\text{env}} = 0$ .

Another major source of imperfections is the information loss from the channel. In this case, the propagation relation Eq. (5) can be rewritten as

$$f_{\text{in},j}(t) = \kappa f_{\text{out},j-1}(t - \tau), \quad (22)$$

where we assume that the distance between adjacent nodes is equal, and  $\kappa$  is the total loss rate of the waveguide between node  $j$  and  $j - 1$ . QLEs in this case become

$$\dot{a}_j(t) = - \sum_k \Theta(j - k) \kappa^{j-k} g_j(t) g_k(t) a_k(t). \quad (23)$$

A simulation of the process  $|100\rangle \rightarrow (|010\rangle + |001\rangle)/\sqrt{2}$  when  $\kappa = 0.9$  in the waveguide is shown in Fig. 6(c). Moreover, quantum information may also be lost from the nodes, attributed to the coupling between nodes and the external environment. For numerical simulation, an effective Hamiltonian can be derived to describe the unidirectional connected nodes,

$$H_{\text{eff}} = \sum_j \left[ \hbar\omega_0 a_j^\dagger a_j - i\hbar g_j(t) \sum_k \Theta(j - k) g_k(t) a_j^\dagger a_k \right]. \quad (24)$$

Note that  $H_{\text{eff}}$  is not Hermitian due to the unidirectionality of the system. The loss to the external environment can be simulated with the master equation

$$\begin{aligned} \dot{\rho} = & -\frac{i}{\hbar} (H_{\text{eff}} \rho - \rho H_{\text{eff}}^\dagger) \\ & + \frac{g_{\text{env}}^2}{2} \sum_j [(N_{\text{env}} + 1)(2a_j \rho a_j^\dagger - a_j^\dagger a_j \rho - \rho a_j^\dagger a_j) \\ & + N_{\text{env}}(2a_j^\dagger \rho a_j - a_j a_j^\dagger \rho - \rho a_j a_j^\dagger)], \end{aligned} \quad (25)$$

where  $\rho$  is the density matrix of the subsystem containing all the nodes, and every node couples to the external environment with the same coupling constant  $g_{\text{env}}$ . Here  $N_{\text{env}}$  denotes the thermal number of the environment with respect to the photon frequency  $\omega_0$ . In Fig. 6(d), we simulated the generation of  $(|10\rangle + |01\rangle)/\sqrt{2}$  by considering such loss with  $g_{\text{env}} = g_{\text{max}}/10$ . The loss of quantum information from the channel or nodes can be reduced by improving the quality of the devices, or using suitable error-correction methods [65,66].

#### V. FEASIBILITY

In this section, we discuss the feasibility of this protocol in terms of two kinds of quantum systems: artificial atoms (superconducting circuits) and natural atoms ( $\Lambda$ -type atoms).

### A. Artificial atoms

The superconducting system is one promising candidate to implement this protocol, where superconducting qubits or oscillators can be utilized as the universal nodes while the superconducting transmission line or coaxial waveguide acts as the channel. In practice, using a coupler commonly composed of superconducting quantum interference devices (SQUIDs) or flux qubits to connect a superconducting qubit and a waveguide, the tunable coupling can be achieved by applying time-dependent microwave driving fields [67–71]. A modulation of the coupling strength from 0 to 100 MHz has been verified in experiments [67]. Thus, different pulse shapes of  $g_i(t)$  in our protocol can be accessible by tuning coupling strengths.

Besides the tunability of the coupling, we also need to be capable of synthesizing the required initial state shown in Sec. III in order to prepare the state of the emitter in the protocol. Currently, microwave driving fields are often utilized to synthesize an arbitrary quantum state in a cavity. For instance, if a cavity is coupled to a transmon, we can apply a series of driving fields to the transmon so as to manipulate the phase of different Fock states and then create an arbitrary state [72]. If the transition frequency of the qubit is tunable, we can also combine the modulation of the transition frequency with some series of driving fields to prepare arbitrary states [73].

In the last two years, two-node transfer and the entanglement preparation protocol have been realized in superconducting circuits [35,38]. A transfer-process fidelity of  $85.8\% \pm 0.06\%$  has been achieved and entanglement with a fidelity of  $75.3\% \pm 0.1\%$  successfully generated. Our protocol is based on similar experimental requirements as the two-node one; the experimental realizations of the two-node protocol therefore ensure the feasibility of our protocol. By analogy with the setup in the experiments mentioned above, we show a possible superconducting quantum circuit design for the one-dimensional network with  $N$  nodes in Fig. 7(a).

### B. Natural atoms

Natural atomic systems, such as three-level atoms or doping defects [47,74–76], can also serve as nodes in this protocol. By applying external driving fields, the three-level system can reduce to an effective two-level system with a tunable coupling. For example, one can apply an adjustable driving field, with Rabi frequency  $\Omega(t)$ , to implement time-dependent control of the electronic ground state of a silicon-vacancy (SiV) center embedded in the diamond cantilever [47,77,78], as shown in Fig. 7(b). Here the SiV center, with a  $\Lambda$ -type level structure, can be regarded as a two-level system through a Raman process, where the population of the stable state  $|2\rangle$  can coherently convert into a propagating phonon of the cantilever. Consequently, a tunable coupling [approximately  $\Omega(t)\Gamma(\omega)/\delta_0$ ] between

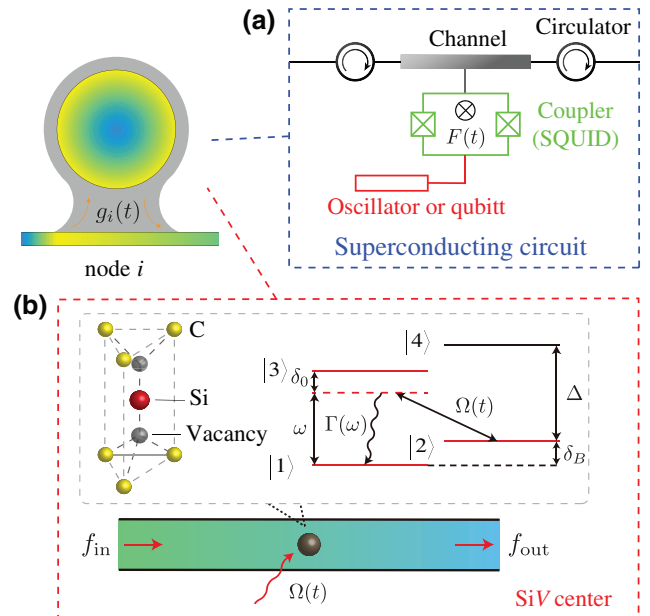


FIG. 7. Two examples of the node-channel system. (a) Schematic diagram of a possible quantum network composed of superconducting circuits. By tuning  $F(t)$ , which is a magnetic flux through the SQUID, a time-dependent coupling strength  $g(t)$  can be realized. (b) Schematic of a SiV center coupled to the waveguide. The coupling strength is controlled by a microwave driving field with time-dependent Rabi frequency  $\Omega(t)$ .

the SiV center and the acoustic mode can be effectively obtained. Note that one can employ the collective mode of an ensemble of effective two-level atoms (or defects) as the node, which can be approximately regarded as a harmonic oscillator when the number of atoms is sufficiently large [24]. In our protocol, the process to initialize the state of atomic systems is also important, which could be realized by applying pumpings or laser cooling [79–81]. For example, Ref. [79] used an optical pulse to pump the SiV center to the spin-down ground state.

Recently, many works have focused on quantum state transfer in natural atomic systems [82–84]. For instance, taking advantage of phonon-spin couplings in the SiV center system, Lemonde *et al.* [46] proposed a theoretical framework for the quantum network, where SiV centers act as nodes and quantum information can be transferred between them via an acoustic waveguide. These previous studies demonstrate the high feasibility and huge potential of such a multinode quantum network based on time-dependent modulation in future quantum technologies.

## VI. CONCLUSION AND OUTLOOK

We propose a multinode state transfer and preparation protocol in a one-dimensional quantum network with time-dependent couplings. Through the designed modulation of

the coupling strengths between the nodes and their common channel, one can use this protocol to transfer an arbitrary quantum state in the emitter to any node in the receiver or prepare multinode entanglement states. The time-dependent control pulses of couplings are derived under a series of dark-state conditions represented by Eqs. (11) and (12), which are crucial for this protocol. Considering state-of-art technologies, our protocol can be implemented in various experimental platforms, such as vacancy centers in the diamond and superconducting circuits. This protocol exhibits the great capacity of quantum state distribution and nonlocal entanglement preparation, which are the basics for constructing a quantum network. It opens an intriguing door to explore the possibility of performing nonlocal quantum operations in a 1D quantum network with multiple nodes, which may provide technical reserve for the large-scale quantum computation and quantum network.

## ACKNOWLEDGMENTS

This work is supported by the National Natural Science Foundation of China (Grant No. 11874432), the National Key R&D Program of China (Grant No. 2019YFA0308200), and the Science and Technology Planning Project of Guangdong Province (Grant No. pdjh2020b0014). Z.H.P. is supported by the National Science Foundation of China (Grants No. 61833010, No. 12074117, and No. 12061131011).

## APPENDIX A: DERIVATION OF QUANTUM LANGEVIN EQUATIONS

We begin from the Heisenberg equation  $\dot{a}_j = i\hbar^{-1} [H_{\text{total}}, a_j]$  with respect to the system Hamiltonian in Sec. II. Considering a short timescale, we have

$$\begin{aligned}\dot{a}_j &= -i\omega_0 a_j - g_j(\omega_0) \int d\omega B_{\omega,j} e^{-i\omega t} \\ &\quad - g_j^2(\omega_0) \int_0^t ds a_j(t) \delta(t-s).\end{aligned}\quad (\text{A1})$$

By defining  $f_{\text{in},j}$  (shown in Sec. II) and using the properties of the  $\delta$  function, Eq. (3) can be derived. Similarly, we derive the input-output relations with the Heisenberg equation of  $B_{\omega,j}$ , and we have

$$\dot{B}_{\omega,j} = -i\omega B_{\omega,j} + g_j(\omega_0) a_j. \quad (\text{A2})$$

The field near node  $j$  can be expressed with  $B_j(z, t) = \int d\omega \exp(i\omega z/c) B_{\omega,j}$ . So, by integrating Eq. (A2) and taking the limit of  $B_j(z \rightarrow 0^\pm, t)$ , the input-output relations (4) can be obtained.

When the input noise is neglected and the nodes are arranged in sequence, we can obtain the output field of

node  $j$  by iteration,

$$f_{\text{out},j}(t) = f_{\text{in},0}(t) + \sum_{k \leq j} g_k(t) a_k(t), \quad (\text{A3})$$

which is Eq. (6) when the input noise is neglected. By substituting Eq. (6) into Eq. (3), Eq. (7) can be derived.

## APPENDIX B: DERIVATION OF THE PROTOCOL

To derive Eq. (15), we start from the combination of dark-state conditions and the QLE of the  $N$ th node  $\dot{a}_N(t) = \frac{1}{2}g_N^2(t)a_N(t) - g_N(t) \sum_{j=1}^N g_j(t)a_j(t)$ , and we can then obtain

$$\dot{a}_N(t) = \frac{1}{2}g_N^2(t)a_N(t). \quad (\text{B1})$$

Note that the equation above is not a physical evolution equation, it only holds when the dark-state condition is satisfied. According to the time-symmetrical boundary conditions

$$a_N(t_f)/a_0(0) = a_0(t_f)/a_N(0) = c_N, \quad (\text{B2})$$

and the QLE of the first node  $da_0/dt = -\frac{1}{2}g_0^2 a_0$ , we assert that our entanglement preparation protocol can be realized if the two equations share the same form after time reversal,

$$g_0^2(t) = g_N^2(t_f - t). \quad (\text{B3})$$

Equation (6) tells us that the extended dark-state condition is equivalent to  $f_{\text{out},j-1} = D_{j-1,j}/(1 - D_{j-1,j})g_j a_j$ . Substituting it into Eq. (3) of the  $j$ th node, we get

$$\dot{a}_j(t) = \left( \frac{D_{j-1,j}}{D_{j-1,j} - 1} - \frac{1}{2} \right) g_j^2 a_j(t). \quad (\text{B4})$$

After that, we can apply the proportional boundary conditions (14) to the above equation and get Eq. (15).

As for examples, we show the detailed derivation of Eq. (13). Let us begin with the form

$$\dot{a}_j(t) = -\frac{1}{2}g_j(t)(f_{\text{out},j} + f_{\text{out},j-1}) \quad (\text{B5})$$

by combining Eqs. (6) and (7). We then substitute equation Eq. (B5) and  $f_{\text{out},j+1} = f_{\text{out},j}/D_{j+1,j}$  into

$$\dot{a}_j(t) = \frac{c_j}{c_{j+1}} \dot{a}_{j+1}(t). \quad (\text{B6})$$

Equations (12) and (13) can be obtained after that.

Let us derive the pulse shapes of generating a two-node entanglement  $c_1|10\rangle + c_2|01\rangle$  in a three-node network. According to Eq. (13), we have  $1/D_{1,2} = 0$  and

$D_{0,1} = (c_1/c_2)(g_2/g_1) - 1$ . Hence, if  $g_2/g_1 \neq 0$ , Eq. (15) can be simplified to a quadratic equation in  $g_2/g_1$ :

$$\left(\frac{g_2}{g_1}\right)^2 - 2\frac{c_2}{c_1}\frac{g_2}{g_1} - 1 = 0. \quad (\text{B7})$$

Note that  $c_2/c_1$  can be a complex number. Assuming that  $g_j$  is positive, we can solve Eq. (B7) to obtain the exact number of  $g_2/g_1$  as

$$\frac{g_2}{g_1} = \begin{cases} \sqrt{2} + 1 & \text{for } c_1 = c_2 = \frac{1}{\sqrt{2}}, \\ \sqrt{2} - 1 & \text{for } c_1 = -c_2 = -\frac{1}{\sqrt{2}}. \end{cases} \quad (\text{B8})$$

- [1] A. E. Kozhekin, K. Molmer, and E. Polzik, Quantum memory for light, *Phys. Rev. A* **62**, 033809 (2000).
- [2] W. Rosenfeld, S. Berner, J. Volz, M. Weber, and H. Weinfurter, Remote Preparation of an Atomic Quantum Memory, *Phys. Rev. Lett.* **98**, 050504 (2007).
- [3] B. Zhao, Y.-A. Chen, X.-H. Bao, T. Strassel, C.-S. Chuu, X.-M. Jin, J. Schmiedmayer, Z.-S. Yuan, S. Chen, and J.-W. Pan, A millisecond quantum memory for scalable quantum networks, *Nat. Phys.* **5**, 95 (2009).
- [4] A. Reiserer, N. Kalb, M. S. Blok, K. J. M. van Bemmel, T. H. Taminiau, R. Hanson, D. J. Twitchen, and M. Markham, Robust Quantum-network Memory Using Decoherence-protected Subspaces of Nuclear Spins, *Phys. Rev. X* **6**, 021040 (2016).
- [5] Christopher Chudzicki and Frederick W. Strauch, Parallel State Transfer and Efficient Quantum Routing on Quantum Networks, *Phys. Rev. Lett.* **105**, 260501 (2010).
- [6] Peter J. Pemberton-Ross and Alastair Kay, Perfect Quantum Routing in Regular Spin Networks, *Phys. Rev. Lett.* **106**, 020503 (2011).
- [7] Y. Li and S. C. Benjamin, Hierarchical surface code for network quantum computing with modules of arbitrary size, *Phys. Rev. A* **94**, 042303 (2016).
- [8] Y. Zhong, H.-J. Chang, A. Bienfait, É. Dumur, M.-H. Chou, C. R. Conner, J. Grebel, R. G. Povey, H. Yan, D. I. Schuster, and A. N. Cleland, Deterministic multi-qubit entanglement in a quantum network, *Nature (London)* **590**, 571 (2021).
- [9] S. Wehner, D. Elkouss, and R. Hanson, Quantum internet: A vision for the road ahead, *Science* **362**, 303 (2018).
- [10] W. Wang, F. Xu, and H.-K. Lo, Asymmetric Protocols for Scalable High-rate Measurement-device-independent Quantum Key Distribution Networks, *Phys. Rev. X* **9**, 041012 (2019).
- [11] Ian A. Walmsley and Joshua Nunn, Editorial: Building Quantum Networks, *Phys. Rev. Appl.* **6**, 040001 (2016).
- [12] H. J. Kimble, The quantum internet, *Nature (London)* **453**, 1023 (2008).
- [13] J. Biamonte, M. Faccin, and M. D. Domenico, Complex networks from classical to quantum, *Commun. Phys.* **2**, 55 (2019).
- [14] D. Poderini, I. Agresti, G. Marchese, E. Polino, T. Giordani, A. Suprano, M. Valeri, G. Milani, N. Spagnolo, G. Carvalho, R. Chaves, and F. Sciarrino, Experimental violation of  $n$ -locality in a star quantum network, *Nat. Commun.* **11**, 2467 (2020).
- [15] P. Kómár, E. M. Kessler, M. Bishof, L. Jiang, A. S. Sørensen, J. Ye, and M. D. Lukin, A quantum network of clocks, *Nat. Phys.* **10**, 582 (2014).
- [16] M. Brekenfeld, D. Niemietz, J. D. Christesen, and G. Rempe, A quantum network node with crossed optical fibre cavities, *Nat. Phys.* **16**, 647 (2020).
- [17] Matthias Christandl, Nilanjana Datta, Artur Ekert, and Andrew J. Landahl, Perfect State Transfer in Quantum Spin Networks, *Phys. Rev. Lett.* **92**, 187902 (2004).
- [18] M. Röntgen, C. V. Morfonios, I. Brouzos, F. K. Diakonos, and P. Schmelcher, Quantum Network Transfer and Storage with Compact Localized States Induced by Local Symmetries, *Phys. Rev. Lett.* **123**, 080504 (2019).
- [19] Sougato Bose, Quantum Communication through an Unmodulated Spin Chain, *Phys. Rev. Lett.* **91**, 207901 (2003).
- [20] J. I. Cirac, P. Zoller, H. J. Kimble, and H. Mabuchi, Quantum State Transfer and Entanglement Distribution among Distant Nodes in a Quantum Network, *Phys. Rev. Lett.* **78**, 3221 (1997).
- [21] A. Acín, J. I. Cirac, and M. Lewenstein, Entanglement percolation in quantum networks, *Nat. Phys.* **3**, 256 (2007).
- [22] S. Leedumrongwatthanakun, L. Innocenti, H. Defienne, T. Juffmann, A. Ferraro, M. Paternostro, and S. Gigan, Programmable linear quantum networks with a multimode fibre, *Nat. Photonics* **14**, 139 (2020).
- [23] G. F. Peñas, R. Puebla, T. Ramos, P. Rabl, and J. J. García-Ripoll, Universal deterministic quantum operations in microwave quantum links, *arXiv:2110.02092* (2021).
- [24] Z.-L. Xiang, M. Zhang, L. Jiang, and P. Rabl, Intricacy Quantum Communication via Thermal Microwave Networks, *Phys. Rev. X* **7**, 011035 (2017).
- [25] B. Vermersch, P.-O. Guimond, H. Pichler, and P. Zoller, Quantum State Transfer via Noisy Photonic and Phononic Waveguides, *Phys. Rev. Lett.* **118**, 133601 (2017).
- [26] Alexander N. Korotkov, Flying microwave qubits with nearly perfect transfer efficiency, *Phys. Rev. B* **84**, 014510 (2011).
- [27] E. A. Sete, E. Mlinar, and Alexander N. Korotkov, Robust quantum state transfer using tunable couplers, *Phys. Rev. B* **91**, 144509 (2015).
- [28] K. Stannigel, P. Rabl, A. S. Sørensen, M. D. Lukin, and P. Zoller, Optomechanical transducers for quantum-information processing, *Phys. Rev. A* **84**, 042341 (2011).
- [29] R. J. Coles, D. M. Price, J. E. Dixon, B. Royall, E. Clarke, P. Kok, M. S. Skolnick, A. M. Fox, and M. N. Makhonin, Chirality of nanophotonic waveguide with embedded quantum emitter for unidirectional spin transfer, *Nat. Commun.* **7**, 11183 (2016).
- [30] P. Lodahl, S. Mahmoodian, S. Stobbe, A. Rauschenbeutel, P. Schneeweiss, J. Volz, H. Pichler, and P. Zoller, Chiral quantum optics, *Nature (London)* **541**, 473 (2017).
- [31] S. Tan, R. W. Bomantara, and J. Gong, High-fidelity and long-distance entangled-state transfer with Floquet topological edge modes, *Phys. Rev. A* **102**, 022608 (2020).
- [32] F. Mei, G. Chen, L. Tian, S.-L. Zhu, and S. Jia, Robust quantum state transfer via topological edge states in superconducting qubit chains, *Phys. Rev. A* **98**, 012331 (2018).

- [33] C. Dlaska, B. Vermersch, and P. Zoller, Robust quantum state transfer via topologically protected edge channels in dipolar arrays, *Quantum Sci. Technol.* **2**, 015001 (2017).
- [34] M. B. Zanjani, A. R. Davoyan, A. M. Mahmoud, N. Engheta, and J. R. Lukes, One-way phonon isolation in acoustic waveguides, *Appl. Phys. Lett.* **104**, 081905 (2014).
- [35] P. Magnard, S. Storz, P. Kurpiers, J. Schär, F. Marxer, J. Lütolf, T. Walter, J.-C. Besse, M. Gabureac, K. Reuer, A. Akin, B. Royer, A. Blais, and A. Wallraff, Microwave Quantum Link between Superconducting Circuits Housed in Spatially Separated Cryogenic Systems, *Phys. Rev. Lett.* **125**, 260502 (2020).
- [36] L. D. Burkhardt, J. D. Teoh, Y. Zhang, C. J. Axline, L. Frunzio, M. H. Devoret, L. Jiang, S. M. Girvin, and R. J. Schoelkopf, Error-Detected State Transfer and Entanglement in a Superconducting Quantum Network, *PRX Quantum* **2**, 030321 (2021).
- [37] L. Steffen, Y. Salathe, M. Oppliger, P. Kurpiers, M. Baur, C. Lang, C. Eichler, G. Puebla-Hellmann, A. Fedorov, and A. Wallraff, Deterministic quantum teleportation with feed-forward in a solid state system, *Nature (London)* **500**, 319 (2013).
- [38] P. Kurpiers, P. Magnard, T. Walter, B. Royer, M. Pechal, J. Heinsoo, Y. Salathé, A. Akin, S. Storz, J.-C. Besse, S. Gasparinetti, A. Blais, and A. Wallraff, Deterministic quantum state transfer and remote entanglement using microwave photons, *Nature (London)* **558**, 264 (2018).
- [39] C. J. Axline, L. D. Burkhardt, W. Pfaff, M. Zhang, K. Chou, P. Campagne-Ibarcq, P. Reinhold, L. Frunzio, S. M. Girvin, L. Jiang, M. H. Devoret, and R. J. Schoelkopf, On-demand quantum state transfer and entanglement between remote microwave cavity memories, *Nat. Phys.* **14**, 705 (2018).
- [40] K. S. Chou, J. Z. Blumoff, C. S. Wang, P. C. Reinhold, C. J. Axline, Y. Y. Gao, L. Frunzio, M. H. Devoret, L. Jiang, and R. J. Schoelkopf, Deterministic teleportation of a quantum gate between two logical qubits, *Nature (London)* **561**, 368 (2018).
- [41] A. Bienfait, K. J. Satzinger, Y. P. Zhong, H.-S. Chang, M.-H. Chou, C. R. Conner, É. Dumur, J. Grebel, G. A. Peairs, R. G. Povey, and A. N. Cleland, Phonon-mediated quantum state transfer and remote qubit entanglement, *Science* **364**, 368 (2019).
- [42] Amir H. Safavi-Naeini and Oskar Painter, Proposal for an optomechanical traveling wave phonon-photon translator, *New J. Phys.* **13**, 013017 (2011).
- [43] Marc-Antoine Lemonde, Vittorio Peano, Peter Rabl, and Dimitris G. Angelakis, Quantum state transfer via acoustic edge states in a 2D optomechanical array, *New J. Phys.* **21**, 113030 (2019).
- [44] G. D. de Moraes Neto, F. M. Andrade, V. Montenegro, and S. Bose, Quantum state transfer in optomechanical arrays, *Phys. Rev. A* **93**, 062339 (2016).
- [45] S. J. M. Habraken, K. Stannigel, M. D. Lukin, P. Zoller, and P. Rabl, Continuous mode cooling and phonon routers for phononic quantum networks, *New J. Phys.* **14**, 115004 (2012).
- [46] M.-A. Lemonde, S. Meesala, A. Sipahigil, M. J. A. Schuetz, M. D. Lukin, M. Loncar, and P. Rabl, Phonon Networks with Silicon-Vacancy Centers in Diamond Waveguides, *Phys. Rev. Lett.* **120**, 213603 (2018).
- [47] Z. Y. Xu, Y. M. Hu, W. L. Yang, M. Feng, and J. F. Du, Deterministically entangling distant nitrogen-vacancy centers by a nanomechanical cantilever, *Phys. Rev. A* **80**, 022335 (2009).
- [48] Y.-F. Qiao, H.-Z. Li, X.-L. Dong, J.-Q. Chen, Y. Zhou, and P.-B. Li, Phononic-waveguide-assisted steady-state entanglement of silicon-vacancy centers, *Phys. Rev. A* **101**, 042313 (2020).
- [49] Peng-Bo Li, Ze-Liang Xiang, Peter Rabl, and Franco Nori, Hybrid Quantum Device with Nitrogen-Vacancy Centers in Diamond Coupled to Carbon Nanotubes, *Phys. Rev. Lett.* **117**, 015502 (2016).
- [50] C. T. Nguyen, D. D. Sukachev, M. K. Bhaskar, B. Machielse, D. S. Levonian, E. N. Knall, P. Stroganov, R. Riedinger, H. Park, M. Lončar, and M. D. Lukin, Quantum Network Nodes Based on Diamond Qubits with an Efficient Nanophotonic Interface, *Phys. Rev. Lett.* **123**, 183602 (2019).
- [51] P. C. Humphreys, N. Kalb, J. P. J. Morits, R. N. Schouten, R. F. L. Vermeulen, D. J. Twitchen, M. Markham, and R. Hanson, Deterministic delivery of remote entanglement on a quantum network, *Nature (London)* **558**, 268 (2018).
- [52] N. Kalb, A. A. Reiserer, P. C. Humphreys, J. J. W. Bakermans, S. J. Kamerling, N. H. Nickerson, S. C. Benjamin, D. J. Twitchen, M. Markham, and R. Hanson, Entanglement distillation between solid-state quantum network nodes, *Science* **356**, 6341 (2017).
- [53] X.-Y. Zhu, T. Tu, A.-L. Guo, Z.-Q. Zhou, G.-C. Guo, and C.-F. Li, Spin-photon module for scalable network architecture in quantum dots, *Sci. Rep.* **10**, 5063 (2020).
- [54] R. Li, L. Petit, D. P. Franke, J. P. Dehollain, J. Helsen, M. Steudtner, N. K. Thomas, Z. R. Yoscovits, K. J. Singh, S. Wehner, L. M. K. Vandersypen, J. S. Clarke, and M. Veldhorst, A crossbar network for silicon quantum dot qubits, *Sci. Adv.* **4**, 3960 (2018).
- [55] Wang Yao, Ren-Bao Liu, and L. J. Sham, Theory of Control of the Spin-Photon Interface for Quantum Networks, *Phys. Rev. Lett.* **95**, 030504 (2005).
- [56] M. Almendros, J. Huwer, N. Piro, F. Rohde, C. Schuck, M. Hennrich, F. Dubin, and J. Eschner, Bandwidth-Tunable Single-Photon Source in an Ion-Trap Quantum Network, *Phys. Rev. Lett.* **103**, 213601 (2009).
- [57] S. Ritter, C. Nölleke, C. Hahn, A. Reiserer, A. Neuzner, M. Uphoff, M. Mücke, E. Figueroa, J. Bochmann, and G. Rempe, An elementary quantum network of single atoms in optical cavities, *Nature (London)* **484**, 195 (2012).
- [58] J. I. Cirac and P. Zoller, Preparation of macroscopic superpositions in many-atom systems, *Phys. Rev. A* **50**, R2799 (1994).
- [59] W. Dür, G. Vidal, and J. I. Cirac, Three qubits can be entangled in two inequivalent ways, *Phys. Rev. A* **62**, 062314 (2000).
- [60] P. Kómár, T. Topcu, E. M. Kessler, A. Derevianko, V. Vuletić, J. Ye, and M. D. Lukin, Quantum Network of Atom Clocks: A Possible Implementation with Neutral Atoms, *Phys. Rev. Lett.* **117**, 060506 (2016).
- [61] It is the same for harmonic oscillators and two-level systems when the whole process involves only a single photon or excitation. In this work, only Sec. III C does not work for two-level systems, and the different thermal properties

- of harmonic oscillators and two-level systems are discussed in Sec. IV.
- [62] C. W. Gardiner, Driving a Quantum System with the Output Field from Another Driven Quantum System, *Phys. Rev. Lett.* **70**, 2269 (1993).
- [63] C. W. Gardiner and M. J. Collett, Input and output in damped quantum systems: Quantum stochastic differential equations and the master equation, *Phys. Rev. A* **31**, 3761 (1985).
- [64] The receiver state is  $|\Phi'\rangle$  and all nodes are measured with detectors of  $2\omega_0$ , the detectors may respond (each with probability 1/6), and the quantum state would collapse to  $|02\rangle$  or  $|20\rangle$  because of a nonlinear process. However, if the detectors do not respond, the quantum state would collapse to  $|\Phi^\pm\rangle$  (with a probability of 2/3).
- [65] Emanuel Knill, Raymond Laflamme, and Lorenza Viola, Theory of Quantum Error Correction for General Noise, *Phys. Rev. Lett.* **84**, 2525 (2000).
- [66] M. H. Michael, M. Silveri, R. T. Brierley, V. V. Albert, J. Salmilehto, L. Jiang, and S. M. Girvin, New Class of Quantum Error-correcting Codes for a Bosonic Mode, *Phys. Rev. X* **6**, 031006 (2016).
- [67] M. S. Allman, F. Altomare, J. D. Whittaker, K. Cicak, D. Li, A. Sirois, J. Strong, J. D. Teufel, and R. W. Simmonds, rf-SQUID-Mediated Coherent Tunable Coupling between a Superconducting Phase Qubit and a Lumped-Element Resonator, *Phys. Rev. Lett.* **104**, 177004 (2010).
- [68] S. J. Srinivasan, A. J. Hoffman, J. M. Gambetta, and A. A. Houck, Tunable Coupling in Circuit Quantum Electrodynamics Using a Superconducting Charge Qubit with a *V*-Shaped Energy Level Diagram, *Phys. Rev. Lett.* **106**, 083601 (2011).
- [69] M. Pechal, L. Huthmacher, C. Eichler, S. Zeytinoğlu, A. A. Abdumalikov, Jr., S. Berger, A. Wallraff, and S. Filipp, Microwave-controlled Generation of Shaped Single Photons in Circuit Quantum Electrodynamics, *Phys. Rev. X* **4**, 041010 (2014).
- [70] S. Zeytinoğlu, M. Pechal, S. Berger, A. A. Abdumalikov, Jr., A. Wallraff, and S. Filipp, Microwave-induced amplitude- and phase-tunable qubit-resonator coupling in circuit quantum electrodynamics, *Phys. Rev. A* **91**, 043846 (2015).
- [71] P. Forn-Díaz, J. J. García-Ripoll, B. Peropadre, J.-L. Orgiazzi, M. A. Yurtalan, R. Belyansky, C. M. Wilson, and A. Lupascu, Ultrastrong coupling of a single artificial atom to an electromagnetic continuum in the nonperturbative regime, *Nat. Phys.* **13**, 39 (2017).
- [72] Reinier W. Heeres, Brian Vlastakis, Eric Holland, Stefan Krastanov, Victor V. Albert, Luigi Frunzio, Liang Jiang, and Robert J. Schoelkopf, Cavity State Manipulation Using Photon-Number Selective Phase Gates, *Phys. Rev. Lett.* **115**, 137002 (2015).
- [73] Max Hofheinz, H. Wang, M. Ansmann, Radoslaw C. Bialczak, Erik Lucero, M. Neeley, A. D. O'Connell, D. Sank, J. Wenner, John M. Martinis, and A. N. Cleland, Synthesizing arbitrary quantum states in a superconducting resonator, *Nature (London)* **459**, 546 (2009).
- [74] I. Buluta, S. Ashhab, and F. Nori, Natural and artificial atoms for quantum computation, *Rep. Prog. Phys.* **74**, 104401 (2011).
- [75] P. Treutlein, P. Hommelhoff, T. Steinmetz, T. W. Hansch, and J. Reichel, Coherence in Microchip Traps, *Phys. Rev. Lett.* **92**, 203005 (2004).
- [76] P. Neumann, N. Mizuochi, F. Rempp, P. Hemmer, H. Watanabe, S. Yamasaki, V. Jacques, T. Gaebel, F. Jelezko, and J. Wrachtrup, Multipartite entanglement among single spins in diamond, *Science* **320**, 1326 (2008).
- [77] K. V. Kepesidis, M.-A. Lemonde, A. Norambuena, J. R. Maze, and P. Rabl, Cooling phonons with phonons: Acoustic reservoir engineering with silicon-vacancy centers in diamond, *Phys. Rev. B* **94**, 214115 (2016).
- [78] Yi-Fan Qiao, Hong-Zhen Li, Xing-Liang Dong, Jia-Qiang Chen, Yuan Zhou, and Peng-Bo Li, Phononic-waveguide-assisted steady-state entanglement of silicon-vacancy centers, *Phys. Rev. A* **101**, 042313 (2020).
- [79] Lachlan J. Rogers, Kay D. Jahnke, Mathias H. Metsch, Alp Sipahigil, Jan M. Binder, Tokuyuki Teraji, Hitoshi Sumiya, Junichi Isoya, Mikhail D. Lukin, Philip Hemmer, and Fedor Jelezko, All-Optical Initialization, Readout, and Coherent Preparation of Single Silicon-Vacancy Spins in Diamond, *Phys. Rev. Lett.* **113**, 263602 (2014).
- [80] B. Pingault, D.-D. Jarausch, C. Hepp, L. Klintberg, J. N. Becker, M. Markham, C. Becker, and M. Atatüre, Coherent control of the silicon-vacancy spin in diamond, *Nat. Commun.* **8**, 15579 (2017).
- [81] D. A. Golter, T. Oo, M. Amezcuá, K. A. Stewart, and H. Wang, Optomechanical Quantum Control of a Nitrogen-Vacancy Center in Diamond, *Phys. Rev. Lett.* **116**, 143602 (2016).
- [82] Zhang-qí Yin and Fu-li Li, Multiatom and resonant interaction scheme for quantum state transfer and logical gates between two remote cavities via an optical fiber, *Phys. Rev. A* **75**, 012324 (2007).
- [83] A. Dantan and M. Pinard, Quantum-state transfer between fields and atoms in electromagnetically induced transparency, *Phys. Rev. A* **69**, 043810 (2004).
- [84] J. Q. You and F. Nori, Atomic physics and quantum optics using superconducting circuits, *Nature (London)* **474**, 589 (2011).